Author's Accepted Manuscript

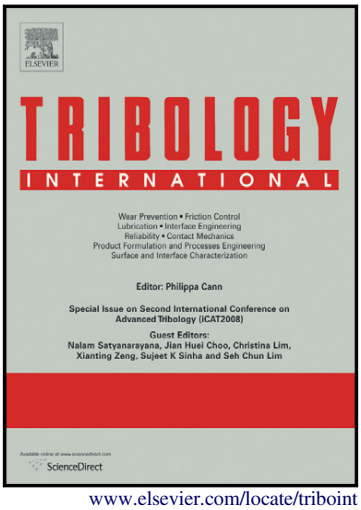

www.elsevier.com/locate/triboint

Engine Oil Acidity Detection Using Solid State Ion Selective Electrodes

M. Soleimani, M. Sophocleous, M. Glanc, J. Atkinson, L. Wang, R.J.K. Wood, R.I. Taylor

PII: S0301-679X(13)00081-9
DOI: http://dx.doi.org/10.1016/j.triboint.2013.02.030
Reference: JTRI3003

To appear in: *Tribology International*

Received date: 9 August 2012
Revised date: 15 February 2013
Accepted date: 18 February 2013

Cite this article as: M. Soleimani, M. Sophocleous, M. Glanc, J. Atkinson, L. Wang, R.J. K. Wood, R.I. Taylor, Engine Oil Acidity Detection Using Solid State Ion Selective Electrodes, *Tribology International,* http://dx.doi.org/10.1016/j.triboint.2013.02.030

This is a PDF file of an unedited manuscript that has been accepted for publication. As a service to our customers we are providing this early version of the manuscript. The manuscript will undergo copyediting, typesetting, and review of the resulting galley proof before it is published in its final citable form. Please note that during the production process errors may be discovered which could affect the content, and all legal disclaimers that apply to the journal pertain.

ACCEPTED MANUSCRIPT

ENGINE OIL ACIDITY DETECTION USING SOLID STATE ION SELECTIVE ELECTRODES

M. Soleimani[a, *], M. Sophocleous[a], M. Glanc[a], J. Atkinson[a], L. Wang[a], R.J.K. Wood[a], R. I. Taylor[b]

[a]Faculty of Engineering & the Environment, University of Southampton, UK
[b]Shell Global Solutions (UK), Cheshire Innovation Park, Chester, UK

Keywords: Lubricating oil, Deterioration, Chemical Degradation, Condition monitoring, oil acidity, Thick-Film, pH Sensor

Abstract

Lubricating oil of moving parts is a critical factor for the performance and longevity of cars and industrial engines. The lubricant degradation occurring during application can be detrimental to the proper operation of lubricated machines if the oil is not changed in a timely manner. However, the oil degradation process is often influenced by a number of parameters, such as the operating temperature and contamination. This offers a challenge to oil monitoring technologies. This study investigates the feasibility of detecting changes in oil acidity using Ion Selective Electrodes (ISE) fabricated using thick-film (TF) screen printing technology. The working electrode is a TF Ruthenium Oxide (RuO_2) ISE; the reference electrodes are three different types of TF reference electrodes and commercial glass pH reference electrode. Artificially degraded oil samples from oxidation tests and model oils produced by adding acid have been used for the evaluation of the sensors. Acid Number (AN) of all oil samples was obtained using conventional titration method. The results show that the TF electrodes responded linearly to the change in oil acidity under different temperatures. Their sensitivity in detecting oil acidity in the model oils is found to be much higher than that of the commercial electrode. Initial analysis also shows that the sensor responses decrease as the temperature increases.

1. Introduction

Engine oil quality monitoring has attracted considerable interest over the years since lubrication is a critical factor for the performance and longevity of cars and industrial engines. In order to maximise engine efficiency and extend useful life, lubricant oil change intervals should be optimised.

Oil quality decreases due to oxidation and contamination, such as debris, fuel and coolant dilution etc[1]. At low levels water solubilises in oil and can react with lubricating additives to reduce their effectiveness, while at higher contents it forms an emulsion which can decrease viscosity[2]. Fuel and glycol contaminants can dilute oil leading to a reduction in viscosity. High levels of soot and other combustion by-products produce colloidal suspension which can increase the oil viscosity. Oxidation produces undesirable by-products such as aldehydes and acidic compounds (weak acids e.g. carboxylic acids) that may cause corrosion and lead to varnish and sludge formation[3].

Formulated lubricating oils consist of a base oil with additives to reduce oxidation rates. However once the additives are consumed the performance of the oil will rapidly decrease threatening the life of the machine.

Oil condition monitoring techniques monitor oil properties to make a quality assessment. A number of physical and electrical properties, such as viscosity and conductivity, have been employed to monitor the level of oil contamination and oxidation, while chemical properties, such as composition and acidity/alkalinity, are particularly used to assess oil degradation due to oxidation.

Currently the most popular oil condition monitoring practice is still based on off-line debris analysis. Real-time accurate oil condition monitoring, that can provide timely information on oil condition, is still in deman[4]. A number of techniques, for measuring oil physical properties, such as Quantitative Debris Monitor (QDM) sensor[5], Cambridge viscosity sensors[6], PAJ water-in-oil sensor[7] and the Tan-delta dielectric sensor[8], TEMIC QLT-Sensor[9], and solid state oscillating crystal devices including flexural[10] and acoustic wave[11] sensors are being developed. The TEMIC QLT-sensor measures the dielectric constant of lubricant and together with other engine parameters, oil condition is predicted. Daimler Benz and Shell have developed indirect or algorithm based techniques based on engine parameters such as rotation speed and driving habit to estimate the optimal mileage for oil changes[12,13].

Accepted manuscript

Due to the complexity in oil chemistry, there have not been any reliable on-line sensors for oil chemical property monitoring. Typically, oil acidity is quantified by the acid number (AN) and base number (BN). Acid number, as a measure of strong inorganic (e.g. nitric acid) and weak organic acids (e.g. carboxylic acid) has been widely used as an indicator of oil acidity and oxidation conditions[14]. Weak acids are produced in the course of oxidation, while strong acids are produced during engine combustion[15]. The acidity of oils depends on the amount of both weak acid, e.g. carboxylic acids, and strong acids, e.g. nitric and sulphuric acid. The level of strong acids significantly affects the corrosiveness of the oil and the level of weak acids has also effects on oil viscosity. Fresh oils with full package of additives tend to be slightly basic (or alkali) due to the presence of overbased detergents. Over the time, the detergents react with acidic by-products from oil oxidation and the oil becomes more and more acidic. To evaluate oil conditions, both AN and BN values of an oil are measured at certain time intervals. As the oil ages, AN value increases while its BN value decreases[16]. It is recommended, by a number of engine and lubricant manufacturers, that the oil should be changed when the AN equals the BN values[17,18,19].

Attempts in miniaturising infrared (IR)[20] sensor for oil chemical monitoring have been reported, however, little success is achieved so far. Smiechowskia et al developed an Iridium oxide sensor for non-aqueous solutions such as industrial lubricants[21]. Although a good correlation between the sensor outputs and the AN/BN was found when tested with diesel oils, the sensitivity and stability of the sensors are quite poor. Price et al.[22] developed an electrochemical probe consisting of three coated platinum and silver wire electrodes for extracting electroactive species into the polymer for monitoring oil additives (e.g. amine antioxidants) in turbine lubricants. Their results, based on voltammetric responses, were promising in measuring oil additives quantitatively, but the electrodes suffer from reliability (e.g. temperature dependency) and durability issues.

Dickert et al[23,24,25] developed a mass sensitive Quartz Crystal Microbalance (QCM) sensor to detect acidic by-products in engine oil. The QCM sensor was coated with molecularly imprinted polyurethanes and ceramic sol-gel layers as well as nanoscale-patterned. They demonstrated that the frequency of the QCM changes proportionally with the changes in molecularly imprinted cavities as a result of acidic by-products of oil degradation absorbed onto the sensor. But, the contaminants of the oil such as fuel, can affect the signal output.

Solid state ion selective electrodes using thick film technologies, introduced over fifty years ago, have shown good sensing capabilities in pH measurements for aqueous solutions. However, their feasibility of detecting engine oil acidity has yet to be explored.

2. Thick-film technology

TF technology was initially introduced as an alternative method for interconnections and networks of passive components because it allows for the reliable and compact production of printed circuit boards through hybridisation[26]. Other techniques emerged for designing printed circuit boards which overcome the benefits of TF technology but it was realised that TF technology can be used in the development of planar solid state sensors[27]. Thick film sensors allow flexible design, offering a wide range of materials with closely controlled parameters and provide low cost infrastructure and mass production opportunity. They are small, robust with a good reproducibility and require minimal treatment[28,29,30].

Many types of TF sensors have been reported within the past years, including physical, chemical and electrochemical sensors[31,32,33,34]. The low cost of the TF sensors allows for disposable sensors which are widely used in biochemical analysis as biosensors[31].

Thick-film technology consists of the sequential screen printing and firing of inks onto a substrate. Ceramic substrates such as alumina are most commonly used while flexible carbon substrates have also been reported[35]. Inks are printed layer by layer on the substrate and each paste serves a specific property. A wide range of conducting, resistive, capacitive and insulating pastes are commercially available. The conductive pastes, made of a binding agent (glasses in powder form, resins, and cellulose acetate), solvent (terpineol, ethylene glycol, cyclohexanone), vehicle (ethylcellulose, which controls viscosity of the pastes during printing due to its thixotropic properties) and additives that determine functional characteristics, are the active parts of the sensors[36]. The binding agent is

Accepted manuscript

the ingredient that once fired will melt and re-solidify and bond with the substrate or the underlying paste. Solvents are used to dissolve the binders in order for the ink to be in the liquid form. They evaporate during the drying process. Vehicles are the ones responsible for the ink's viscosity and are used to make the liquid into a printable ink. They start off thick but become thinner as they are sheared by the printing process. This enables them to flow through the screen mesh better but still retain their paste like properties when not being sheared. Additives are the active materials such as silver or gold for conductive pastes[36]. The main steps of the screen printing are printing, drying (at about 150°C) and firing at the specific firing temperature of the ink used.

2.1 pH theory

pH sensors typically employ potentiometric measurement in aqueous solutions. The sensor consists of two electrodes, a pH ISE, and a silver/silver-chloride (Ag/AgCl) reference electrode. The reference electrode is required to have a stable potential while the ion selective electrode (i.e. the working electrode) responds to the change of the H^+ concentration in the solution. In this study, a ruthenium oxide (RuO_2) ISE coupled with a silver/silver chloride (Ag/AgCl) reference electrode has been selected to investigate the feasibility of measuring acidity levels in lubricating oils. RuO_2 working electrode has been demonstrated to have the highest sensitivity to pH changes compared to any other metal oxide tested[37]. Ag/AgCl reference electrodes maintain their potential because of the establishment of a stable equilibrium in the reversible reaction taking place at the surface of the electrode[38,39,40,41].

Ion selective electrodes such as ruthenium oxide electrodes used here were explained by Fog and Buck[42,43] to undergo the following reaction:

$$MO_n + 2\delta H^+ + 2\delta e^- \leftrightarrow MO_{n-\delta} + \delta H_2 \quad (4)$$

Where MO_n is the higher oxidation state metal oxide and $MO_{n-\delta}$ is the lower oxidation state. The potential for this reaction is given by:

$$E = \left(\frac{RT}{F}\right) \ln a_{H^+}^{1} + \left(\frac{RT}{F}\right) \ln a_{\delta} + \text{constant} \quad (5)$$

Another possible mechanism was suggested of only one redox reaction between two insoluble ruthenium oxides:

$$RuO_2 \cdot 2H_2O + H^+ + e^- \leftrightarrow H_2O + Ru(OH)_3 \quad (6)$$

Where $RuO_2 \cdot 2H_2O$ is the nominal composition of hydrated ruthenium dioxide and $Ru(OH)_3$ is the hydrated ruthenium sesquioxide also written as $RuO_2 \cdot 3H_2O$. The potential of the reaction at a nominal room temperature of 25°C is given by:

$$E = E_0 - 0.0591pH \quad (7)$$

Where, E_0 is the standard potential of the cell. Theory predicts a sensitivity of 59mV/pH. In practice, Thick-Film ruthenium oxide electrodes show an almost Nernstian response of 56mV/pH[37].

2.2 Thick film electrode fabrication

Three types of TF reference electrodes were used in these experiments. The first type was just bare silver conductor while the other two types had an extra layer of Ag/AgCl, one with polymer based binder and one glass based. Lastly a commercial gel-filled Ag/AgCl reference electrode (Beckman Coulter A57193) was also used.

The Thick-Film electrodes used were screen-printed onto 50 mm x 50 mm, 0.625 mm thick, 96% alumina substrates (Coorstech) where each substrate was divided into six equal sized electrodes and pre-scribed with laser lines so that each electrode could be easily snapped off along those lines. Thus, six electrodes were fabricated simultaneously (see Figure 1(left)).

The electrodes were constructed by successive screen-printing of each separate layer. The screen

Accepted manuscript

designs for each layer were produced using AUTOCAD to give precise dimensions of the mesh openings. Each screen was designed to print a single layer of the electrode. The first layer was the silver conductor so the mesh opening was a rectangle with dimensions of 2.25 mm x 44.55 mm. Secondly; a dielectric layer was deposited on top of the silver layer, leaving a small window opening exposing the underlying silver. The screen mesh opening had a rectangular shape of 6.5 mm x 43.8 mm. The window size was 3.4 mm x 3.4 mm square while a part of the underlying layer approximately 4.15 mm x 2.25 mm was exposed for soldering of connecting wires, as shown in Figure 1(right).

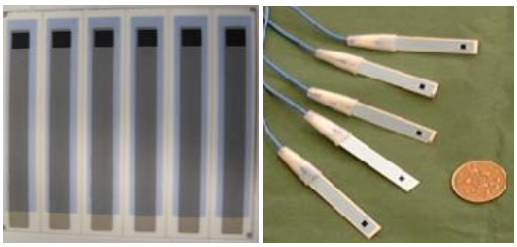

Figure 1 (left): RuO_2 thick-film pH electrodes, (right): electrodes wiring

Next, the screen for the Ag/AgCl layer was a square window of 4 mm x 4 mm, slightly bigger than the exposed silver making sure all the silver was covered. The first three screens were made from stainless steel with 250 lines/inch, 45^o mesh and were manufactured for the Aurel C880 Printer by MCI, Cambridge. The silver conductor layer was printed using ESL-9912 ink and on top of this, dielectric insulator ESL 4905-C was deposited to protect the conductor from the electrolyte.
The construction procedure as explained, mimics the construction of the single junction glass gel-filled Ag/AgCl commercial reference electrode. Two types of Ag/AgCl were used, a polymer based ink provided by Gwent Electronic Materials (GEM C61003P7) while the other type was glass based ink provided by Universidad de Politécnica de Valencia in Spain (PPCFB2). The glass bound silver/silver chloride paste was prepared as follows. PPCFB2 - AgCl (Aldrich 227927) milled to 400 rpm/30min with ethanol (Pulverisette Fritsch), sieve/100µm, Ag (Aldrich 32708-5) sieve/100µm, powder frit (Ferro EG2020VEG) sieve/100µm, vehicle -solvent (Heraeus V-006), mixed in the ratios 3g Ag + 3g AgCl + 2g frit + 3.84g vehicle and triple roll milled for 5 minutes.
For the pH electrode construction, three different inks were used. The first layer was the conductor which was Platinum Gold (ESL 5837) and was screen printed on the same type of substrates, with the same screen as the silver conductor layer for the reference electrodes, with exactly the same procedure. For the second layer a polymer dielectric insulating paste was used (GEM 2020823D2) with the same screen as the one used for the dielectric insulator for the reference electrodes. On top of that, over the window exposing the conductor, a Ruthenium Oxide paste was printed (C505502D7) as the sensitive material for the H+ concentration. The screen used for this layer was the same as the one used for the Ag/AgCl layer of the reference electrodes. A typical construction of a pH electrode is shown in Figure 2.
After the printing process for each layer the electrodes were held at room temperature for 10 minutes to allow relaxation of surface stresses and then dried in an infrared mini dryer (DEK 1209). The layers that required 850°C firing were fired in a 6 zone belt furnace (BTU VQ41) at a peak temperature of 850°C with an ascent and decent temperature of 50°C/min keeping it at peak for 10 minutes. Drying and curing temperatures for each paste are provided in Table 1.

3. Experimental details

The TF Ruthenium oxide pH electrode was used as the working electrode and was connected to a high input impedance (~tera ohm) voltmeter, Metrohm 827 pH lab, together with three types of thick-film reference electrodes and a commercial reference electrode in order to measure the potential difference in oils. Different types of reference electrodes were tested in order to compare and select the most suitable for oil acidity measurments. Details of all reference electrodes used are

Accepted manuscript

shown in Table 2.

Layer	Paste	Drying temperature (°C)	Drying time (min)	Curing temperature (°C)	Curing time (min)
Platinum Gold Conductor	ESL 5837	125	10– 15	850	~45
Dielectric polymer insulator	GEM 2020823D2	-	-	80	30
Ruthenium oxide	C50502D7	-	-	80	10 □ 15
Silver conductor	ESL-9912-A	125	10 □ 15	850	~45
Dielectric insulator	ESL-4905-C	125	10 □ 15	850	~45
Polymer silver - silver chloride	GEM C61003P7	-	10	60	30
Glass silver - silver chloride	PPCFB2	150	10	390	~30

Table 1: Drying and curing temperatures for pastes used

Reference Electrodes	Name	Description
1	Commercial	**Commercial Beckman Coulter**
2	TF Glass	**Silver (ESL9912-A), Dielectric layer (ESL4905-C), Glass Silver-Silver Chloride**
3	TF Bare Ag	**Silver (ESL9912-A), Dielectric layer (ESL4905-C(**
4	TF Polymer	**Silver (ESL9912-A), Dielectric layer (ESL4905-C), Polymer Silver-Silver Chloride**

Table 2: Reference electrodes used for the experiments

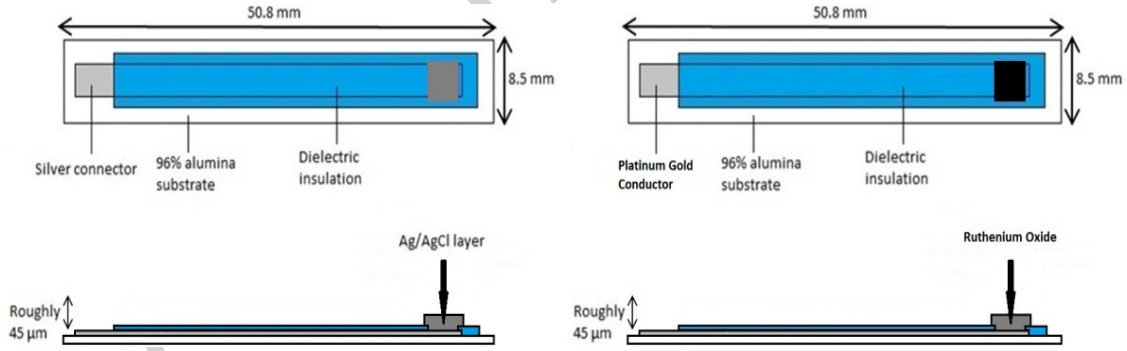

Figure 2: Cross sectional view through a thick film reference electrode (left), and the RuO2 pH electrode as working electrode (right)

All electrode pairs were hydrated and tested in aqueous buffer solutions to determine the baseline response of the TF sensors and confirm their functionality. Hydration time for the electrodes, i.e. the period after which the electrodes produce stable potentials, was determined by monitoring them in pH 7 buffer solution for two hours taking readings every five minutes. The sensors were then immediately cyclically tested in three buffer solutions (pH= 4, 7 and 10) prior to being tested in oil samples. The Beckman Coulter commercial reference electrode was also tested for comparison. Readings were taken every five minutes for each working-reference electrode pair in each oil for five times and the average and standard error were then calculated.

The electrodes were tested in oil samples at two oil temperatures controlled by a water bath, as

illustrated in Figure 3.

3.1 The oil samples

To evaluate the TF electrodes, two sets of oil samples were prepared, where the first set of oil samples were prepared by progressively adding nitric acid drops (30% concentration, Fisher Scientific) into a fresh engine oil (off-shelf Magnatec Fully Synthetic SAE 5W30). Nitric acid was used in the first set as it replicates combustion by-product. There are five oil samples in this set and the details of the acid concentrations are given in Table 3. To ensure the acid mixes well in the oil, the oil was constantly stirred while the acid drops were added into the oil for 15 minutes before the responses from the electrodes were recorded. No significant changes in the appearance of the oil were observed after the addition of acid.

The oxidised oil samples in set 2 came from a proprietary in-house Blown NOx (BNOX) oxidation test carried out at Shell's Houston laboratories. During oxidisation, 350 ml of a Motiva Star 6 base oil (a group II base oil containing no additives) were heated to a temperature of 155°C, whilst an air/NO_2 mixture (NO_2 concentration was 3000 ppm) was passed into the oil at 200 cc/min. A range of samples were taken with varying degrees of oxidation (Table 3). All oil samples were tested at two temperatures at 50 and 80°C (±1˚C) in a thermostatically controlled water-bath (Figure 3). These temperature where designed to simulate the engine environment.

3.2 Acid Number (AN) measurements

In order to validate the performance of the thick film electrodes, Acid Number (AN) of the oil samples was measured using a Kittiwake test kit (Multi-parameter FG-K1-110-KW) at room temperature, following 'ASTM D974 – 12' standard, using colour-indicator titration. This was carried out by adding titrant to a small amount of oil sample (1mL) and observing the colour change of the oil. AN was then calculated based on the number of titrant drops added to the oil sample.

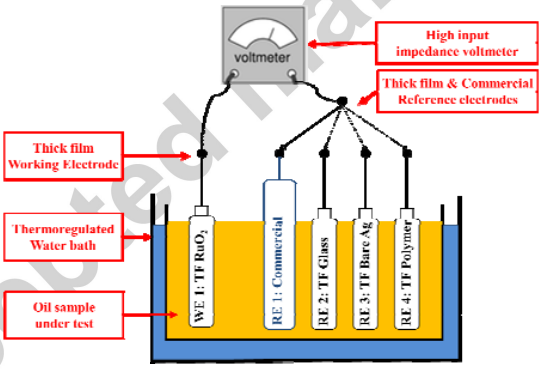

Figure 3: Schematic of the experimental setup for oil acidity measurement

4. Results and discussion

4.1 Hydration and pH testing in buffer solutions

Figure 4 shows the results from the hydration and pH testing at room temperature (i.e. 20°C) using the three types of TF reference electrodes and the commercial reference electrode against the TF RuO_2 working electrode.

From the hydration results (Figure 4 left), it can be seen that all electrodes stabilised within two hours of hydration. The commercial electrode stabilised very quickly while it took at least 40 minutes for the TF reference electrodes to be stabilised. Amongst the three types of TF reference electrodes, the glass electrode stabilised the quickest while the other two took nearly 100 minutes to become stabilised. This is normal with most solid state electrodes and a reason why they generally have to be supplied pre-hydrated. Furthermore, different electrode types stabilised at different potentials due to the differences in the construction, structure and materials of the electrodes.

The results from the pH testing in buffer solutions (see Figure 4 right) show that both the commercial and the TF reference electrodes responded extremely well to the pH changes in the buffer solutions and a linear relationship was found for all the pairs (sensors), see the sensor response vs. pH plots in Figure 5. The slopes (or sensitivities) for the commercial, the TF Glass, TF Polymer and TF Bare Ag REs when paired with RuO_2 WE are 60.2, 51.3, 54.1 and 35.6 mV/pH respectively. Thus the commercial RE exhibited close to an ideal Nernstian behaviour while the TF Glass and Polymer REs also showed near Nernstian responses. The Bare Ag RE slightly underperformed in this respect.

The fact that the commercial RE provided very consistent outputs during both the hydration and cyclic testing in pH buffer solutions demonstrates that the TF RuO_2 WE, paired with all the REs in this study, also performed very consistently.

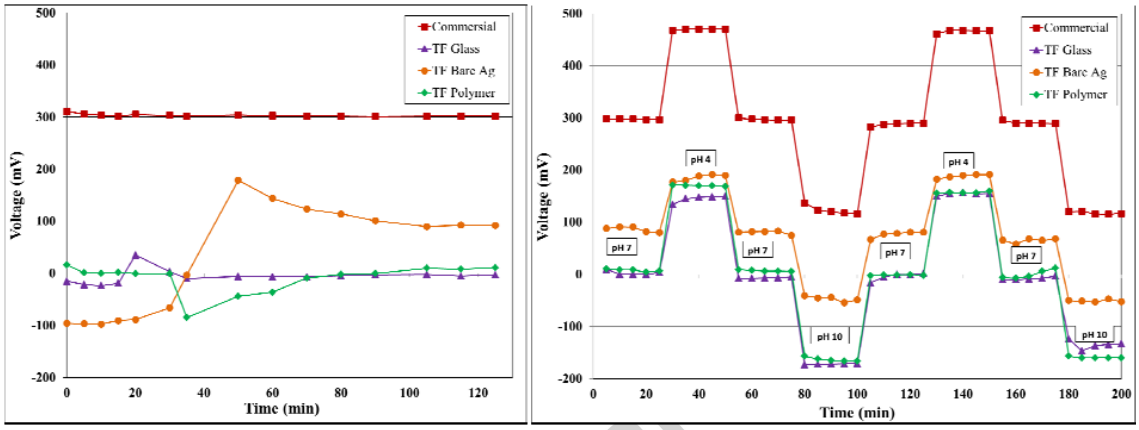

Figure 4: Responses in buffer solutions, (left): hydration response of different thick film electrodes in aqueous buffer solution (pH 7), (right): working electrode vs. respective reference electrodes in different pH buffer solutions

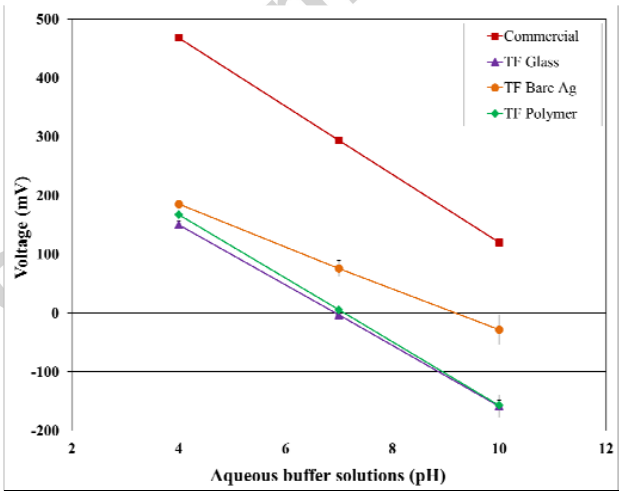

Figure 5: Data from pH testing for each electrode pair

Set 1	Concentration of Acid (ppm)	Acid number (mgKOH/g)	Set 2	Oxidised (hours)	Acid number (mgKOH/g)	Viscosity at 50°C (cSt)
Oil 1	0	0	**Oil 1**	0	0	36.59
Oil 2	100	1	**Oil 2**	2	0.2	38.49
Oil 3	200	1.3	**Oil 3**	4	3.4	51.41
Oil 4	300	1.6	**Oil 4**	16	8.2	68.38
Oil 5	400	1.3	**Oil 5**	20	3.5	95.40

Table 3: Degraded oil samples for the experiments

4.2 Sensor responses in the set 1 oils

The sensor responses in the set 1 oil samples at 50˚C and 80˚C are shown in Figure 6, where the AN values of the oils measured at room temperature are also shown.

For acid concentrations between 100 and 300 ppm, the commercial and the TF REs all increase linearly with the increase of the acid concentration. For acid concentrations between 0 (fresh oil) and 100 ppm, the commercial electrode shows a large decrease while the TF electrodes all show different degrees of increases. As the acid concentration increases above 300 ppm, all sensors show a decrease trend except the TF Bare Ag electrode where a plateau is seen. The linear trend between 100 and 300 ppm for the sensors indicates that the TF electrodes have good potential to be used for oil acidity detection in this range. A different trend in low acid concentrations may be a result that the acid was neutralised by the basic additives (e.g. the detergent) in the oil used in this experiment. The reason for the decrease/plateau in the electrode responses when acid concentration is over 300 ppm is not yet clear and more experiments will be conducted to explore these in the future work. However, it is interesting to see that the AN values initially increase with the acid concentration (between 0 and 300 ppm) but decreased when that is over 300 ppm, i.e. follow a similar trend as the sensors under both temperatures. The sensor responses have been plotted against the AN values of the oils under the two temperatures in Figure 7. The values for 400 ppm acid are not shown since they have same AN values as the 200 ppm acid concentration oil samples but different sensor outputs (causing confusions if plotted on the same graph). It can be seen that the AN values have changed from 0 for the fresh oil to 1.6 mgKOH/g for the oil sample with 300 ppm acid. A linear relationship is found for all electrodes (commercial and the TF) under both temperatures between 1 and 1.6 mgKOH/g. However, this trend doesn't extend to the fresh oil where the AN value is zero. Overall, the sensor responses at 80˚C are lower than that at 50˚C. This will be further discussed in the temperature effects section below.

The sensitivities of the electrodes (mV/AN) under the two temperatures for this set of oils are shown in Table 4. As can be seen, the TF Glass electrode has the highest sensitivity of 254.7 mV/AN at 50˚C while the TF Bare Ag electrode has the highest sensitivity of 177.4 mV/AN at 80˚C. The commercial and TF Polymer electrodes show the lowest sensitivities in monitoring acidity for the set 1 oils.

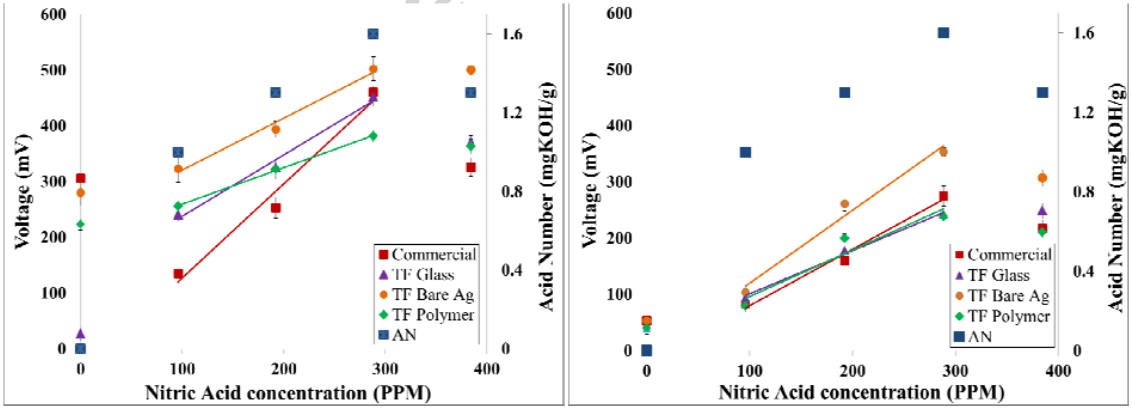

Figure 6: RuO_2 working electrode vs. various reference electrodes in set 1 oil samples, left: at 50°C and right: at 80°C

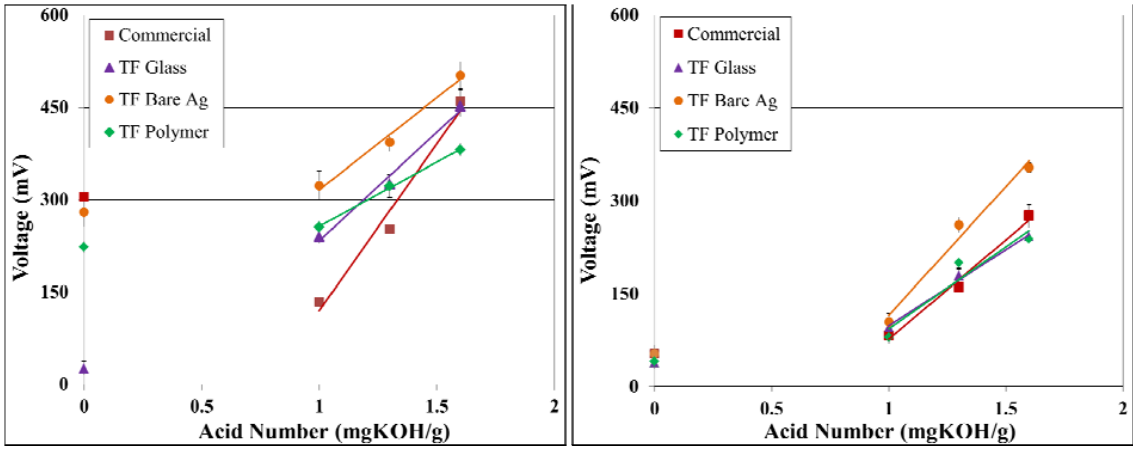

Figure 7: Comparison of thick-film electrodes output vs. AN values set 2 oil samples, left: at 50°C and right: at 80°C

4.3 Sensor responses in the set 2 oils

Responses from the sensors in the second set of oil samples under 50 ˚C and 80˚C have been plotted against the oxidation hours of the oils, see Figure 8. Under both temperatures, an increase in the sensor responses is seen as the oxidation time increases to 16 hours, however a decrease occurs between 16 and 20 hours. To investigate the relationship between the sensor responses and the acidity of the oil samples, the AN values of the oxidised oil samples were measured under room temperature. Figure 9 presents the plots of sensor responses vs. AN values of the oxidised oils. Again, the last points in Figure 9, i.e. the 20-hour oxidisation oil, are not plotted in this figure due to overlapping with a lower oxidisation hour oil of four hours. A much large AN range (between 0 and 8.5 mgKOH/g) is seen in the oxidised oils in set 2 than that of the oils in set 1. This might be due to the differences in the oil types, i.e. set 1 oils are fully formulated oils and set 2 oils are base oils. Also, the acidic contents in the two sets of oils are very different, e.g. a strong acid in set 1 oils and weak acids from oxidation in set 2 oils.

At 50˚C (Figure 9 left), a near linear relationship between the sensor responses and the AN values is seen, which is similar to that of the set 1 oils. However, this relationship is not found for the oxidised oils measured at 80˚C (Figure 9 right). Also, the sensor outputs in oils at 50˚C (between 220 and 340 mV) are generally much higher than those at 80˚C (between -700 and 200 mV). This is considered as a result of the reduction in oil viscosity and the increase conductivity under a higher temperature.

The linear sensitivity of all the sensors are calculated for the range at 50˚C, see Table 4. This was not possible for the 80 ˚C measurements due to the non-linear relationship between the sensor responses and AN values of the oils. It can be seen that all sensors appear to have a sensitivity of about 12 mV/AN at 50 ˚C, where the commercial electrode performed slightly better than the TF electrodes.

4.3 Temperature effects

Figure 10 shows the sensor responses of all the sets 1 and 2 oil samples under the two temperatures (left for set 1 oils and right for set 2 oils) measured by the TF Glass RE coupled with the TF RuO_2 WE.

Generally the sensor responses involving TF REs are lower at 80˚C compared to those at 50˚C. This contradicts the Nernst equation whereby pH sensitivity should increase with increasing temperature and tends to suggest that the TF reference electrodes are experiencing a change in characteristic as a result of the change in temperature. This is further substantiated when comparing the sensitivity of the pH electrode versus the commercial liquid filled RE, which does indeed increase with temperature from 52 mV/AN at 50˚C to 120 mV/AN at 80˚C for set 1 oils. Other factors such as increased oil conductivity and reduced oil viscosity when the temperature was increased from 50 to

Accepted manuscript

80˚C could also have a bearing on the TF RE response. These phenomena will require further investigation over a wider range of temperatures in order to fully understand the sensors' temperature sensitivity and are planned as future work.

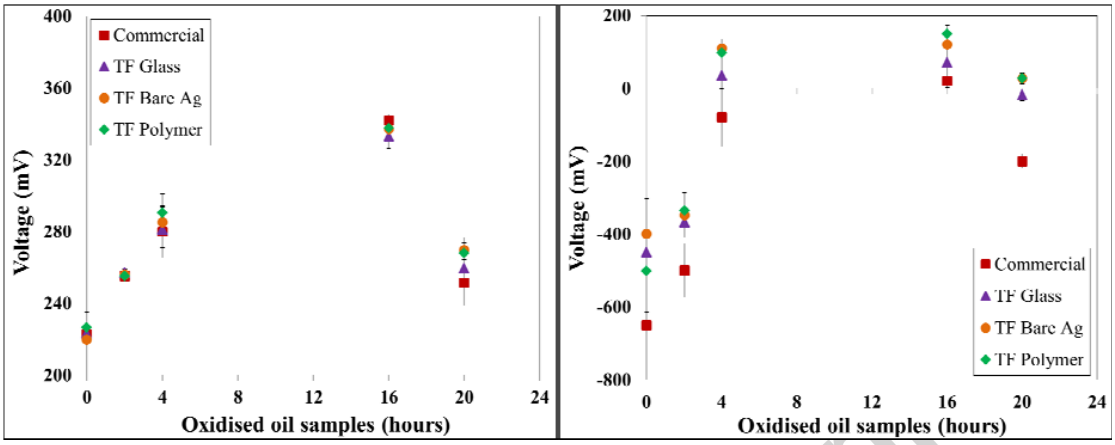

Figure 8: RuO2 working electrode vs. various reference electrodes in set 2 oil samples, left: at 50°C and right: at 80°C

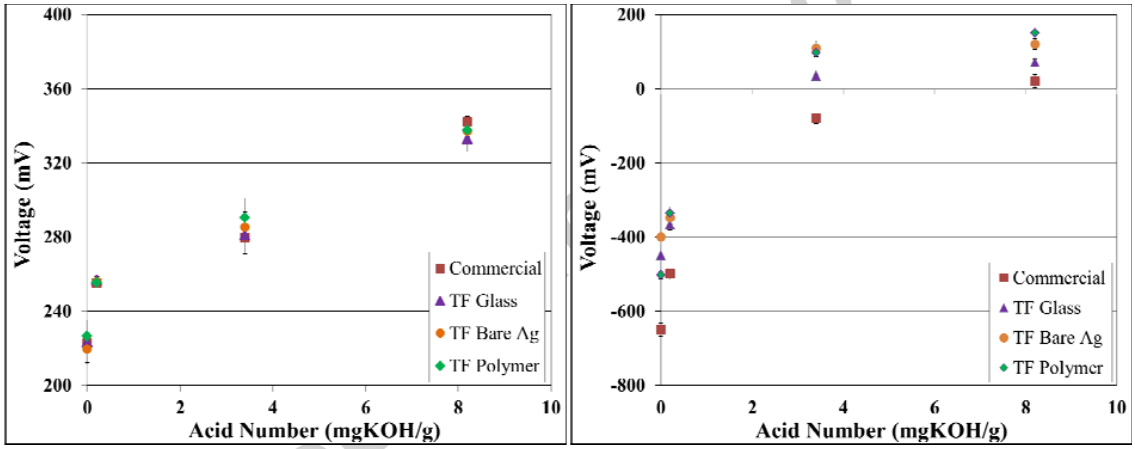

Figure 1: Comparison of thick-film electrodes output vs. AN values of set 2 oil samples, left: at 50°C and right: at 80°C

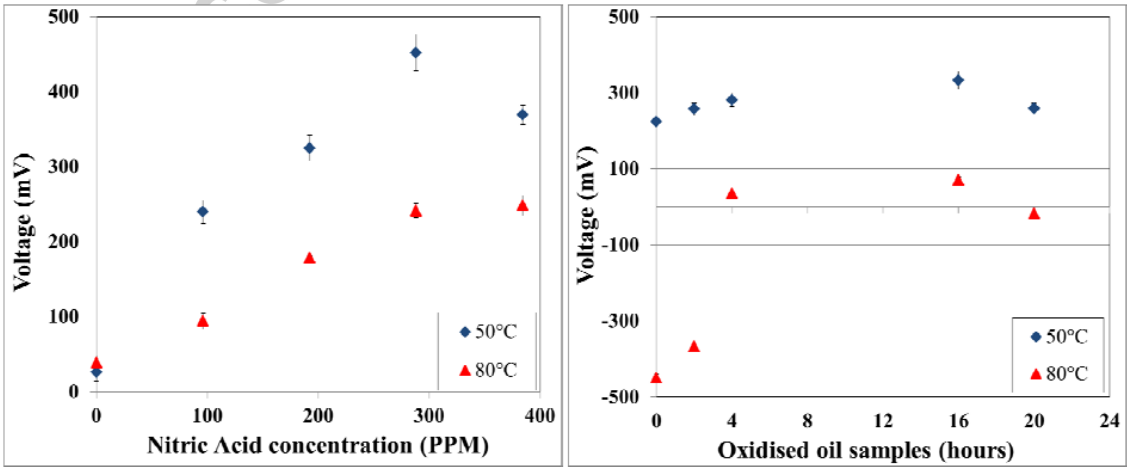

Figure 10: Temperature effect on the output of the TF electrodes: RuO2 working electrode vs. TF Glass reference electrode in set 1 oil samples (left), and set 2 oil samples (right) at two temperatures (50°C and 80°C)

ACCEPTED MANUSCRIPT

	Commercial	Glass	Bare Ag	Polymer
Set 1 oil samples:				
Sensitivity (at 50°C) – [mV/AN]	52	254	122	91
Sensitivity (at 80°C) – [mV/AN]	120	120	177	121
Set 2 oil samples:				
Sensitivity (at 50°C) – [mV/AN]	12	11	12	12

Table 4: Sensitivity of the reference electrodes

5. Conclusions

The feasibility of oil acidity detection using solid state ion selective electrodes has been studied in various oils. Two methods are adapted in producing oils with defined acidity, i.e. thermally oxidising a base oil and adding nitric acid progressively to a fresh fully formulated oil. A RuO_2 TF WE has been coupled with one commercial glass pH RE and three different types of TF REs to investigate their behaviour in oils under two different temperatures. The preliminary conclusions are:

- All three types of TF REs show a linear response to the change of acid contents in set 1 oils between 100 and 300 ppm at both 50 and 80˚C. A linear relationship was also found between the sensor responses and the acid number (AN) measurements in the same range. Although the TF sensors responded linearly to the AN values of the set 2 oils at 50 ˚C, no linearity between them is found at 80 ˚C.
- The TF sensors show higher sensitivity in set 1 oils compared to that of the commercial RE paired with the TF RuO_2 WE. However, their sensitivities in set 2 oils at 50˚C are found to be similar and much lower than those in set 1 oils. This is possibly due to the differences in the acid contents in the two sets of oils, i.e. a strong acid in set 1 oils and weak acids in set 2 oils.
- Further investigation will be carried out to investigate the stability of TF electrodes and their behaviour over a wider range of temperatures.

Acknowledgements

The authors would like to thank Shell Global Solutions for funding this project.

Highlights

- The feasibility of oil acidity detection using screen printed thick-film (TF) electrodes has been studied.
- The TF electrodes responded well to acid contents in both sets of oil samples (mostly linear relationship).
- Temperature effects were also studied by testing the samples at different temperatures.
- It was shown that higher temperatures decrease the sensor outputs.

References

[1] Needleman WM, Madhavan PV. Review of lubricant contamination and diesel engine wear. SAE Tech. Pap. 881827: 1988; doi:10.4271/881827.
[2] Smiechowski MF, Lvovich VF. Electrochemical monitoring of water-surfactant interactions in industrial lubricants. J Electroanal

Accepted manuscript

Chem: 2002; 534 (2): 171-180.
[3] Mortier RM, Fox MF. Orszulik ST. Chemistry and Technology of Lubricants. 3rd ed. New York: Springer; 2009.
[4] Roylance BJ, Hunt TM. The Wear Debris Analysis Handbook. Oxford: Caxmoor Publication Company; 1999.
[5] Maurice LB, et al. Magnetic debris monitoring using magneto-optic sending. U.S. Patent 5,214,377 B1: 1993.
[6] Accessed May 2012: http://www.cambridgeviscosity.com/process-sensors
[7] Accessed May 2012:
http://www.paj.dk/english/Cases/Water-In-Oil-sensor.asp
[8] Accessed May 2012: http://www.tandeltasystems.com/products-oqs.php
[9] Irion E, Land K, Klein M. Oil-Quality Prediction and Oil-Level Detection with the TEMIC QLT-Sensor. SAE Tech. Pap. 970847: 1997; DOI: 10.4271/970847.
[10] Matsiev LF. Application of Flexural Mechanical Resonators to Simultaneous Measurements of Liquid Density and Viscosity. Proc. IEEE Ultrason. Symp.: 1999; Vol. 1: 457–460.
[11] Andle JC. Measurement, Compensation and Control of Equivalent Shear Rate in Acoustic Wave Sensors. U.S. Patent No. 7,181,957: 2007.
[12] Frend M, et al. Extended oil drain intervals– Conservation of resources or reduction of engine life. SAE Tech. Pap. 951035: 1995; DOI: 10.4271/951035.
[13] Frend M, et al. Extended oil drain intervals – Conservation of resources or reduction of engine life (Part II). SAE Tech. Pap. 981443: 1998; DOI: 10.4271/981443.
[14] ASTM D974 -12 Standard Test Method for Acid and Base Number by Colour-Indicator Titration. Accessed May 2012: http://www.astm.org/Standards/D4739.htm
[15] Clark RJ, Fajardo C M. Assessment of the Properties of Internal Combustion Engine Lubricants Using an Onboard Sensor. Tribol. Trans. 2012; 55: 458-465.
[16] Clark RJ, Fajardo C M. Assessment of the Properties of Internal Combustion Engine Lubricants Using an Onboard Sensor. Tribol. Trans. 2012; 55: 458-465.
[17] Sutton M, Stow C. Preliminary studies of the impact of diesel fuel sulphur on recommended oil service interval. Intern. Conf. on Automotive Tech.: 2004; 131-135.
[18] Clark RJ, Fajardoa CM. Assessment of the properties of internal combustion engine lubricants using an onboard sensor. Tribol. Trans. 2012; 55: 458-465.
[19] Polaris Laboratories. Optimizing Drain Intervals Using TBN vs. TAN. Practicing Oil Analysis Magazine: 2008.
[20] Agoston A, Ötsch C, Zhuravleva J, Jakoby B. An IR-Absorption Sensor System for the Determination of Engine Oil Deterioration. Proc. of IEEE Sensors conf. 2004; 1: 463-466.
[21] Smiechowskia MF, Lvovich VF,. Iridium oxide sensors for acidity and basicity detection in industrial lubricants. Sensor Actuat. B-Chem. 2003; 96: 261-267.
[22] Price RJ, Clarke LJ. Chemical sensing of amine antioxidants in turbine lubricants. Analyst 1991; 116: 1121-1123.
[23] Dickert FL, Greibl W, Rohrer A, Voigt G. Sol-Gel-Coated Quartz Crystal Microbalances for Monitoring Automotive Oil Degradation. Adv. Mater. 2001; 13, 17: 1327-1330
[24] Dickert FL, Forth P, Lieberzeit PA, Voigt G. Quality control of automotive engine oils with mass-sensitive chemical sensors-QCMs and molecularly imprinted polymers, J. Anal. Chem. 2000; 366(8), 802–806.
[25] Dickert F, Hayden O, Lieberzeit P, Palfinger C, Pickert D, Wolff U, Scholl G. Borderline applications of QCM-devices: synthetic antibodies for analytes in both nm- and µm dimensions. Sens Actuators B Chem. 2003; 95(1–3):20-24
[26] Prudenziati M and Morten B. The State of the Art in Thick-film Sensors. Microelectr. J. 1992: **23**: 133-141.
[27] Haskard MR and Pitt K. Thick-Film technology and Applications. Electrochemical Publications. 1997.
[28] Topfer ML. Thick-film microelectronics: fabrication, design and applications. Van Nostrand Reinhold Co. 1971.
[29] Brignell PJE, White NM and Cranny AWJ. Sensor applications of thick-film technology. IEEE Proc. 1988; 135:77-84.
[30] Atkinson JK, et al. Screen Printed Thick Film Subterranean and Subaqueous Environmental Chemical Sensor Arrays. 13th EPTC Conf. 2011; 245-250.
[31] Guidi V, et al. Gas sensing through thick film technology. Sensor Actuat. B-Chem. 2002; **84**: 72-77.
[32] Guth U, Vonau W and Zosel J, Recent developments in electrochemical sensor application and technology-a review. Meas. Sci. technol. 2009; **20**(4): 042002.
[33] Galán-Vidal CA, et al. Chemical sensors, biosensors and thick-film technology. Trac-trend anal. Chem. 1995; **14**(5): 225-231.
[34] Martínez-Máñez R., et al. A multisensor in thick-film technology for water quality control. Sensor Actuat. A-Phys. 2005; 120(2): 589-595.
[35]Tarr M. [cited 23/01/2013]; Available from: http://www.ami.ac.uk/courses/topics/0255_tft/index.html.
[36]Loasby RG. Handbook of Thick Film Technology. 1976: Electochemical Publications.
[37] Mihell JA, Atkinson JK. Planar thick-film pH electrodes based on ruthenium dioxide hydrate. Sensor Actuat. B-Chem. 1998; 48: 505-511.
[38] Ives DJG and Janz GJ, Reference Electrodes: Theory and Practice. Academic Press. 1961.
[39] Cranny AWJ and Atkinson JK, Thick film silver-silver chloride reference electrodes. Meas. Sci. technol. 1998; **9**: 1557-1565.
[40] Tymeckia Ł, Zwierkowskab E and Konckia R. Screen-printed reference electrodes for potentiometric measurements. Anal. Chim. Acta 2004; **526**: 3-11.
[41] Atkinson JK, et al. An investigation into the effect of fabrication parameter variation on the characteristics of screen-printed thick-film silver/silver chloride reference electrodes. Microelectronics Int. 2011; **28**(2): 49-52.
[42] Fog A, Buck R. Electronic semiconducting oxides as pH sensors. Sensor Actuat. 1984; 5: 137-146
[43]Glanc-Gostkiewicza M., et al. Performance of miniaturised Thick-Film solid state pH sensors. Proc. Eurosensors 2012; 1299-1302.

Accepted manuscript